NO and N_2O Release from the Trityl Diazeniumdiolate Complexes $[M(O_2N_2CPh_3)_3]^-$ (M = Fe, Co)

Miguel Á. Baeza Cinco, Arunavo Chakraborty, Camilo F. Guzman, Sabrina Kräh, Guang Wu, Trevor W. Hayton*

Department of Chemistry and Biochemistry, University of California, Santa Barbara, Santa Barbara, CA 93106 (USA).

Supporting Information Placeholder

ABSTRACT: Reaction of MBr_2 with 3 equiv of $[K(18\text{-crown-6})][O_2N_2CPh_3]$ generates the trityl diazeniumdiolate complexes $[K(18\text{-crown-6})][M(O_2N_2CPh_3)_3]$ (M = Co, **2**; Fe, **3**) in good yields. Irradiation of **2** and **3** using 371 nm light led to NO formation in 10 and 1% yields (calculated assuming a maximum of 6 equiv of NO produced per complex), respectively. Also formed in the photolysis of **2** was N_2O in 63% yield, whereas photolysis of **3** led to formation of N_2O, as well as $Ph_3CN(H)OCPh_3$, in 37 and 5% yields, respectively. These products are indicative of diazeniumdiolate fragmentation via both C–N and N–N bond cleavage pathways. In contrast, oxidation of complexes **2** and **3** with 1.2 equiv of $[Ag(MeCN)_4][PF_6]$ led to N_2O formation but no NO formation, suggesting that diazeniumdiolate fragmentation occurs exclusively via C–N bond cleavage under these conditions. While the photolytic yields of NO are modest, they represent a 10- to 100-fold increase compared to the previously reported Zn congener, suggesting that the presence of a redox-active metal center favors NO formation upon trityl diazeniumdiolate fragmentation.

INTRODUCTION

Given the far-ranging biological effects of nitric oxide,[1–7] NO-releasing molecules have received intense interest as potential therapeutics.[8–10] Many classes of NO delivery molecules have been studied, including *S*-nitrosothiols,[11,12] *C*-nitroso compounds,[13,14] metal nitrosyl complexes,[15–20] organic nitrites and nitrates,[21,22] *N*-diazeniumdiolates (*N*-DAZDs),[9,10,23] and *C*-diazeniumdiolates (*C*-DAZDs).[23–33] Among these examples, *C*-DAZDs are probably the least explored for their NO-releasing properties. Indeed, only a handful of *C*-DAZDs have been quantitatively examined for NO release,[34–37] which typically release NO via thermolysis or protonation. For example, diazeniumdiolated idazoxan releases NO in 10% yield upon standing at physiological temperature and pH.[38] Similarly, *N*-(4-methoxybenzyl)guanidinium diazeniumdiolate and *N*-(4-nitrobenzyl)guanidinium diazeniumdiolate release NO at pH = 3 in 45 and 20% yields, respectively.[30,39] However, many *C*-DAZDs do not release NO at all (they release N_2O instead),[23,40] or they release NO only very slowly.[28,34] *C*-DAZDs can also function as ligands, and several *C*-DAZD metal complexes have been reported over the years, including $[Cu(O_2N_2Ph)_2]$ and $[Ce(O_2N_2Nap)_3]$ (Nap = naphthyl), among others.[37,41–44] Generally speaking, however, these complexes are not well characterized and, more importantly, their NO-releasing properties remain virtually unexplored.

Recently, we reported the synthesis of the zinc trityl diazeniumdiolate complex, $[K(18\text{-crown-6})][Zn(O_2N_2CPh_3)_3]$ (**1**).[37] The incorporation of the redox-active trityl group into its *C*-diazeniumdiolate ligand was intended to facilitate NO release by encouraging C–N bond cleavage, a necessary step in the release of both equivalents of NO. Although C–N bond cleavage was observed upon both photolysis and oxidation of **1**, only trace amounts of NO were observed in the reaction mixtures, and only in the case of the photolysis reaction. Given these results, we sought to improve the yields of NO by ligation of the trityl diazeniumdiolate to a redox-active metal, which we hypothesized could intercept potential NO-scavenging intermediates generated during the reaction. One such intermediate, $[ONNO]^{\bullet-}$, is known to react rapidly with NO to form N_2O and NO_2^-.[45–47] Herein, we report the synthesis and characterization of two transition metal trityl diazeniumdiolate complexes, namely $[K(18\text{-crown-6})][M(O_2N_2CPh_3)_3]$ (M = Co, Fe), as well as their response to photolytic and oxidative stimuli.

RESULTS AND DISCUSSION

Synthesis of $[K(18\text{-crown-6})][M(O_2N_2CPh_3)_3]$ (M = Co, Fe). Addition of a blue THF solution of $CoBr_2$ to a colorless slurry of 3 equiv of $[K(18\text{-crown-6})][O_2N_2CPh_3]$ in THF afforded a peach suspension, from which $[K(18\text{-crown-6})][Co(O_2N_2CPh_3)_3]$ (**2**) was isolated in 79% yield as pink-red crystals (Scheme 1). Similarly, reaction of a yellow-brown slurry of $FeBr_2$ with 3 equiv of $[K(18\text{-crown-6})][O_2N_2CPh_3]$ in THF produced a red-orange mixture, from

which [K(18-crown-6)][Fe($O_2N_2CPh_3$)$_3$] (**3**) could be isolated in 73% yield as red-orange crystals. Note that the synthesis of the Zn analogue **1** followed a similar protocol.[37] Complex **2** is insoluble in aliphatic solvents, sparingly soluble in Et_2O, and soluble in benzene, toluene, THF, and CH_2Cl_2. Complex **3** is sparingly soluble in aliphatic solvents, moderately soluble in Et_2O, and soluble in benzene, toluene, THF, and CH_2Cl_2. Both complexes are stable for several days as solids when stored under an inert atmosphere at –25 °C. Additionally, neither **2** nor **3** react with H_2O when dissolved in C_6D_6 (Figures S4, S15).

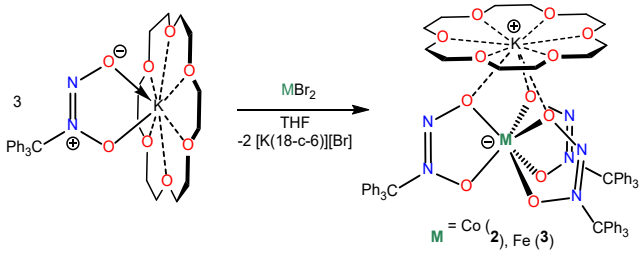

Scheme 1. Synthesis of trityl *C*-DAZD complexes **2** and **3**.

The ^{1}H NMR spectrum of **2** in C_6D_6 features broad resonances at 6.26, 5.62, and 2.28 ppm, assignable to *p*-, *o*-, and *m*-CH environments, respectively. These resonances are present in a 1:2:2 ratio and are indicative of paramagnetism, as expected for an octahedral d^7 complex. Similarly, the ^{1}H NMR spectrum of **3** in C_6D_6 has broad resonances at 12.27 and 7.91 ppm assignable to the *m*- and *o*-CH environments, and another resonance at 7.56 ppm assignable to the *p*-CH environment. These three resonances are present in a 2:2:1 ratio. This spectrum is also indicative of paramagnetism, suggesting a high-spin ground state for this octahedral d^6 complex. Finally, the UV-vis spectrum of complex **2** (1.1 mM) in toluene displays absorption bands at 466 and 550 nm, whereas the UV-vis spectrum of complex **3** (1.0 mM) in toluene shows absorption bands at 341, 366, and 464 nm. These bands can be assigned to LMCT and *d*-*d* transitions and suggest that **2** and **3** will be better suited to photolytic fragmentation than colorless **1**.

Complex **2** crystallized in the monoclinic space group $P2_1/c$ with two independent molecules in the asymmetric unit as the CH_2Cl_2 solvate, **2**·3.5CH_2Cl_2 (Figure 1), while complex **3** crystallized in the monoclinic space group $C2/c$ as the toluene and 18-crown-6 solvate, **3**·2C_7H_8·0.5$C_{12}H_{24}O_6$ (Figure S24). Complexes **2** and **3** are isostructural, and their solid-state structures show the trityl DAZD ligands bound in a *O*,*O*-κ^2 fashion, generating a distorted octahedral geometry around the metal centers.[48] The metrical parameters of the two molecules within the asymmetric unit of **2**·3.5CH_2Cl_2 are similar and only one will be discussed in detail. Complex **2** has Co–O distances ranging from 2.027(5)–2.100(5) Å (Table 1), whereas the Fe–O distances in **3** range from 2.054(6)–2.121(5) Å, both of which compare well with those in **1** (Table 1). The average N–N and C–N distances in **2** (1.28, 1.52 Å) and **3** (1.29, 1.51 Å) are also similar, and are in agreement with those found in **1** (1.27, 1.50 Å) and [Fe(O_2N_2Ph)$_3$] (1.30, 1.42 Å).[43] Complexes **2** and **3** have an average N–O distance of 1.31 Å which also compares well with **1** and [Fe(O_2N_2Ph)$_3$].

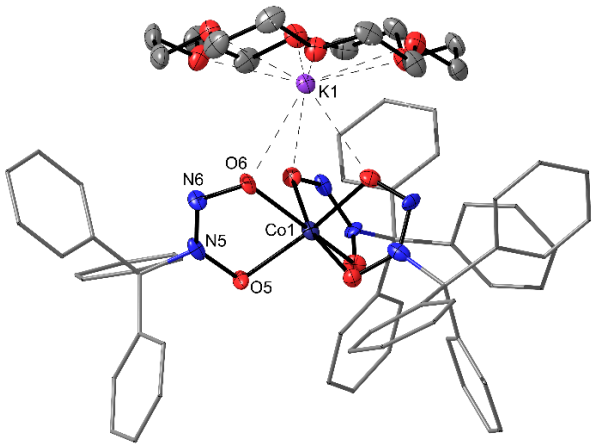

Figure 1. Solid-state structure of **2**·3.5CH_2Cl_2. Thermal ellipsoids drawn at 50% probability. Solvates and hydrogen atoms omitted for clarity.

Table 1. Selected bond lengths and angles (averaged) for **1**, **2**·3.5CH_2Cl_2, and **3**·2C_7H_8·0.5$C_{12}H_{24}O_6$.

Bond/angle	**1**[a]	**2**·3.5CH_2Cl_2	**3**·2C_7H_8·0.5 $C_{12}H_{24}O_6$
M–O_{prox} (Å)[b]	2.049	2.063	2.080
M–O_{dist} (Å)	2.091	2.065	2.107
N_{prox}–O_{prox} (Å)	1.310	1.300	1.314
N_{dist}–O_{dist} (Å)	1.304	1.311	1.296
N_{prox}–N_{dist} (Å)	1.274	1.28	1.288
N_{prox}–C (Å)	1.50	1.52	1.51
O_{prox}–M–O_{dist} (°)	75.2	75.6	73.6

a. Data taken from Ref.[37]

b. O_{prox} denotes the oxygen atoms closest to the trityl substituent, whereas O_{dist} denotes those farthest from it. The same notation is used for nitrogen atoms.

Photolysis of [K(18-crown-6)][M($O_2N_2CPh_3$)$_3$] (M = Co, Fe). As we reported recently,[37] the photolysis of **1** led to NO formation in only trace amounts (Table 2). Also formed during its photolysis was N_2O, as well as the trityl-containing by-products 9-phenylfluorene, Ph_3CH, and $Ph_3CN(H)OCPh_3$. The photolyses of complexes **2** and **3** were examined for comparison. Irradiation of a peach C_6D_6 solution of **2** with a 371 nm LED lightstrip for 20 h resulted in a color change to brown. This photolysis time is dramatically reduced from that of **1**, which reached full conversion only after 9 d, highlighting the better absorption properties of **2**. Analysis of the final mixture by ^{1}H NMR spectroscopy revealed formation of Ph_3CH as the only trityl-containing product (Scheme 2). No $Ph_3CN(H)OCPh_3$ or 9-phenylfluorene were observed in the final mixture,[49,50] although 9-phenylfluorene can be detected during the early stages of the reaction (Figure S5). Similar product distributions were observed upon use of a high pressure Hg lamp (Figure S8). A GC-MS analysis of the reaction headspace revealed N_2O formation in 63% yield (calculated assuming a maximum of 3 equiv of N_2O produced per complex; Figure S25). Additionally, analysis of the reaction headspace using a NO analyzer

revealed the formation of NO in 10% yield (calculated assuming a maximum of 6 equiv of NO produced per complex). The formation of NO in the reaction mixture was further verified by a two-vial trapping experiment with [T(OMe)PP]Co (Figure S7).[51] Despite all our experimental efforts, the fate of the Co ion in this transformation remains unclear.

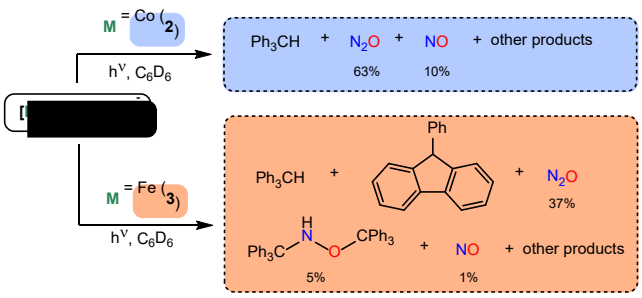

Scheme 2. Photolysis of complexes **2** and **3**.

Photolysis of a red-orange C_6D_6 solution of **3** with a 371 nm LED lightstrip for 6 h produced a color change to ochre. Again, the short photolysis time contrasts with that of **1**, consistent with the better absorption properties of **3**. A ^{1}H NMR spectrum of the final reaction mixture revealed the formation of $Ph_3CN(H)OCPh_3$ in 5% yield (calculated on the basis of NO equivalents). Ph_3CH and 9-phenylfluorene were also observed in this spectrum (Scheme 2).[49,50,52] Their presence in the reaction mixture was further verified via $^{13}C\{^1H\}$ NMR spectroscopy (Figure S17). Similar product distributions were observed upon use of a high pressure Hg lamp (Figure S19). The reaction headspace was analyzed via GC-MS, which showed that N_2O was produced in 37% yield (Table 2, Figure S26). NO was also found in the reaction mixture, in 1% yield according to a NO analyzer experiment (Figure S39). The formation of NO in the reaction mixture was further verified by a two-vial trapping experiment with [T(OMe)PP]Co (Figure S18).[51] Photolysis of **3** with a 478 nm LED lightstrip also results in fragmentation, albeit much more slowly. As with the Co example, the fate of the metal ion in this transformation remains unclear.

Table 2. Observed yields of NO, N_2O, and $Ph_3CN(H)OCPh_3$ (calculated on the basis of NO equivalents) formed upon photolysis of **1**–**3**.

Complex	NO (%)	N_2O (%)	$Ph_3CN(H)OCPh_3$ (%)	Total (%)
1 (Zn)[a]	0.06	51	12	63
2 (Co)	10	63	0	73
3 (Fe)	1	37	5	43

a. Data taken from Ref.[37]

As was seen for complex **1**, the products formed upon photolysis of **2** and **3** provide evidence for competing C–N and N–N bond cleavage pathways. In particular, NO and $Ph_3CN(H)OCPh_3$ are evidently derived from N–N bond homolysis, whereas N_2O, Ph_3CH, and 9-phenyfluorene are derived from C–N bond homolysis. Alternatively, NO could be formed by sequential C–N and N–N bond homolysis reactions, via a hyponitrite intermediate.[53–55] However, there are notable changes in the product distributions between the three complexes (Table 2), which suggest a role for the metal ion in determining the reaction outcome. In particular, **2** and **3** show much improved yields for NO vs. complex **1**. To rationalize this observation, we suggest that the redox active metal can scavenge the hyponitrite radical anion, $[ONNO]^{\bullet-}$, by converting it into $[ONNO]^{2-}$. $[ONNO]^{\bullet-}$ is a plausible intermediate in the reaction (formed by C-N bond homolysis), and a species that is known to react rapidly with NO.[45–47]

Inspection of the total yield of NO equivalents is also informative. Complexes **1** and **2** feature reasonably good NO mass balance, with greater than 60% of the NO equivalents accounted for, but only 43% of the NO equivalents are accounted for in the case of complex **3**. One explanation for this lower yield is the formation of NMR-silent Fe nitrosyl complexes during diazeniumdiolate fragmentation. Evidence to support this hypothesis comes from the solution-phase IR spectrum of the reaction mixture, which features ν_{NO} bands at 1738 and 1682 cm^{-1}. These bands are in the range of those expected for a DNIC.[56–59] For example, $[Fe(PPh_3)_2(NO)_2]$ exhibits ν_{NO} bands at similar energies (1714 and 1668 cm^{-1}).[60] Moreover, the X-band solution-phase EPR spectrum of a photolyzed sample of **3**, recorded at room temperature, reveals a large isotropic peak at g = 2.0315 that is typical of DNICs (Figure S35),[61–65] such as $[PPN][(EtS)_2Fe(NO)_2]$ (g_{iso} = 2.028)[66] and $[PPN][S_5Fe(NO)_2]$ (g_{iso} = 2.03).[67] Also present in the spectrum are less intense signals at g = 2.0005 and g = 2.0182, which we have assigned to an organic-based radical[68–70] and an unknown Fe-containing species, respectively. A ν_{NO} band is also seen in the IR spectrum of the reaction mixture of **2** (1782 cm^{-1}), suggesting that some NO is sequestered by the metal ion in that case, as well,[71,72] although perhaps not in the same quantity. While the yields of NO from **1**, **2**, and **3** are still modest, they represent the first *C*-DAZD metal complexes to be quantitatively examined for photochemical NO release. For comparison, the closely related Fe(III) cupferronate complex $[Fe(O_2N_2Ph)_3]$ also releases NO upon photolysis, but a yield was not reported.[73]

Oxidation of [K(18-crown-6)][M($O_2N_2CPh_3$)$_3$] (M = Co, Fe). We also explored the oxidation chemistry of complexes **2** and **3**. Thus, addition of 1.2 equiv of $[Ag(MeCN)_4][PF_6]$ to a peach CD_2Cl_2 solution of **2** resulted in formation a dark red-brown mixture, concomitant with formation of an insoluble brown solid. Analysis of the reaction mixture by $^{13}C\{^1H\}$ NMR spectroscopy showed the presence of one major trityl-containing product, $O(CPh_3)_2$ (Scheme 3),[37,74] which was formed in 75% yield (calculated on the basis of trityl equivalents; Figure S11). Trace amounts of Ph_3CF were also observed in the reaction mixture, as revealed by a singlet at –126 ppm in the ^{19}F NMR spectrum (Figure S10).[75] Analysis of the reaction headspace by GC-MS revealed the production of N_2O in 53% yield (calculated assuming a maximum of 3 equiv of N_2O produced per complex; Figure S27). However, NO could not be detected in the reaction mixture, as determined by a two-vial trapping experiment with [T(OMe)PP]Co.[51] Additionally, the solution-phase IR spectrum of the mixture does not feature any

bands assignable to ν_{NO} stretches, in contrast to the photolysis of **2** (Figure S33).

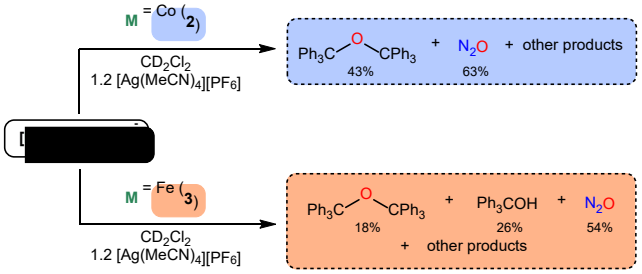

Scheme 3. Oxidation of complexes **2** and **3**.

Addition of 1.2 equiv of $[Ag(MeCN)_4][PF_6]$ to a red-orange CD_2Cl_2 solution of **3** resulted in formation of a deep yellow-brown mixture, concomitant with formation of an insoluble brown solid. The $^{13}C\{^1H\}$ NMR spectrum of the final mixture revealed the presence of $O(CPh_3)_2$ and Ph_3COH as the major trityl-containing products (Scheme 3), in 18% and 26% yield, respectively (calculated on the basis of trityl equivalents; Figure S22). The latter product was evidenced by its characteristic $C_{quaternary}$ resonance at 82.20 ppm.[76] Trace amounts of Ph_3CF were also observed in the ^{19}F NMR spectrum of the reaction mixture. GC-MS analysis of the reaction headspace confirmed N_2O formation in 54% yield (Figure S28). However, no NO was detected in the reaction mixture and, similar to the oxidation of **2**, the IR spectrum of the mixture exhibits no ν_{NO} stretches (Figure S34).

For comparison, a similar product distribution was found for the Zn analogue **1** (Table 3), suggesting that a similar fragmentation mechanism is operative in all three cases; although, it is not immediately clear why Ph_3COH is only observed in the Fe example. Additionally, the observation of N_2O as the sole N-containing product suggests that diazeniumdiolate fragmentation occurs exclusively via heterolytic C–N bond cleavage and loss of trityl cation. This hypothesis is supported by the observation of trace amounts of Ph_3CF in the reaction mixtures, which is likely formed by the partial trapping of $[CPh_3]^+$ by the PF_6^- anion. This mechanism contrasts with that operative in the photolysis reaction, which likely proceeds via homolytic C-N and N-N bond cleavage, potentially explaining the different product distributions.

Table 3. Observed yields of NO, N_2O, $O(CPh_3)_2$, and Ph_3COH formed upon oxidation of **1**–**3**.

Complex	NO (%)	N_2O (%)	$O(CPh_3)_2$ (%)	Ph_3COH (%)
1 (Zn)[a]	0	63	43	0
2 (Co)	0	53	75	0
3 (Fe)	0	54	18	26

a. Data taken from Ref.[37]

CONCLUSIONS

In summary, the transition metal diazeniumdiolate complexes, $[K(18\text{-crown-6})][M(O_2N_2CPh_3)_3]$ (M = Co, Fe), release NO upon photolysis, but not upon oxidation. While the photolytic yields of NO are still modest, they represent a dramatic 10- to 100-fold increase compared to the previously reported Zn congener, suggesting that the presence of redox-active metal center favors NO formation, in line with our original hypothesis. Their yields of NO are also comparable with those reported for other *C*-DAZD-based NO donors.[34,36] Intriguingly, solution-phase IR and EPR data suggest that some NO is trapped by the metal center, suggesting that the yields of NO upon diazeniumdiolate fragmentation are actually higher. Importantly, however, the presence of metal nitrosyl complexes in the reaction mixtures implies that any free NO could be released from a nitrosyl intermediate, and not directly from the DAZD complex, as initially assumed.

ASSOCIATED CONTENT

Supporting Information

The Supporting Information is available free of charge on the ACS Publications website.

Experimental procedures and spectral data for complexes **2** and **3** (CIF, PDF)

Accession Codes

CCDC 2220182 and 2220183 contain the supplementary crystallographic data for this paper. These data can be obtained free of charge via www.ccdc.cam.ac.uk/data_request/cif, or by emailing data_request@ccdc.cam.ac.uk, or by contacting The Cambridge Crystallographic Data Centre, 12 Union Road, Cambridge CB2 1EZ, UK; fax: +44 1223 336033.

AUTHOR INFORMATION

Corresponding Author

* Trevor W. Hayton – Department of Chemistry and Biochemistry, University of California, Santa Barbara, Santa Barbara, California 93106, United States; orcid.org/0000-0003-4370-1424; Email: hayton@chem.ucsb.edu

Authors

Miguel Á. Baeza Cinco – Department of Chemistry and Biochemistry, University of California, Santa Barbara, Santa Barbara, California 93106, United States; orcid.org/0000-0003-2517-4077

Arunavo Chakraborty – Department of Chemistry and Biochemistry, University of California, Santa Barbara, Santa Barbara, California 93106, United States; orcid.org/0000-0001-6325-6511

Camilo F. Guzman – Department of Chemistry and Biochemistry, University of California, Santa Barbara, Santa Barbara, California 93106, United States; orcid.org/0000-0003-0635-7855

Sabrina Kräh – Department of Chemistry and Biochemistry, University of California, Santa Barbara, Santa Barbara, California 93106, United States; orcid.org/0000-0003-3560-2848

Guang Wu – Department of Chemistry and Biochemistry, University of California, Santa Barbara, Santa Barbara, California 93106, United States

ACKNOWLEDGMENT

This work was supported by the National Science Foundation (Grant CHE 2055063). NMR spectra were collected on instruments supported by an NIH Shared Instrumentation grant (Grant 1S10OD012077-01A1). We thank Prof. Peter Ford and Dr. John García for helpful discussions.

REFERENCES

(1) Furchgott, R. F.; Zawadzki, J. V. The Obligatory Role of Endothelial Cells in the Relaxation of Arterial Smooth Muscle by Acetylcholine. *Nature* **1980**, *288*, 373–376.

(2) Ignarro, L. J.; Byrns, R. E.; Buga, G. M.; Wood, K. S. Endothelium-Derived Relaxing Factor from Pulmonary Artery and Vein Possesses Pharmacologic and Chemical Properties Identical to Those of Nitric Oxide Radical. *Circ. Res.* **1987**, *61*, 866–879.

(3) Xu, W.; Liu, L.; Charles, I. G. Microencapsulated INOS-Expressing Cells Cause Tumor Suppression in Mice. *FASEB J.* **2002**, *16*, 1–18.

(4) Cai, T. B.; Tang, X.; Nagorski, J.; Brauschweiger, P. G.; Wang, P. G. Synthesis and Cytotoxicity of 5-Fluorouracil/Diazeniumdiolate Conjugates. *Bioorg. Med. Chem.* **2003**, *11*, 4971–4975.

(5) Bult, H.; Boeckxstaens, G. E.; Pelckmans, P. A.; Jordaens, F. H.; Maercke, Y. M. V.; Herman, A. G. Nitric Oxide as an Inhibitory Non-Adrenergic Non-Cholinergic Neurotransmitter. *Nature* **1990**, *345*, 346–347.

(6) Rand, M. J.; Li, C. G. Nitric Oxide as a Neurotransmitter in Peripheral Nerves: Nature of Transmitter and Mechanism of Transmission. *Annu. Rev. Physiol.* **1995**, *57*, 659–682.

(7) S. Evans, A.; P. Toscano, J. The Chemistry of NO- and HNO-Producing Diazeniumdiolates. In *PATAI'S Chemistry of Functional Groups*; John Wiley & Sons, Ltd, 2010.

(8) Wang, P. G.; Xian, M.; Tang, X.; Wu, X.; Wen, Z.; Cai, T.; Janczuk, A. J. Nitric Oxide Donors: Chemical Activities and Biological Applications. *Chem. Rev.* **2002**, *102*, 1091–1134.

(9) Miller, M. R.; Megson, I. L. Recent Developments in Nitric Oxide Donor Drugs. *Br. J. Pharmacol.* **2007**, *151*, 305–321.

(10) Paul, S.; Pan, S.; Mukherjee, A.; De, P. Nitric Oxide Releasing Delivery Platforms: Design, Detection, Biomedical Applications, and Future Possibilities. *Mol. Pharm.* **2021**, *18*, 3181–3205.

(11) Hogg, N. Biological Chemistry and Clinical Potential of S-Nitrosothiols. *Free Radic. Biol. Med.* **2000**, *28*, 1478–1486.

(12) AL-SA'DONI, H.; FERRO, A. S-Nitrosothiols: A Class of Nitric Oxide-Donor Drugs. *Clin. Sci.* **2000**, *98*, 507–520.

(13) Gooden, D. M.; Chakrapani, H.; Toone, E. J. *C*-Nitroso Compounds: Synthesis, Physicochemical Properties and Biological Activities. *Curr. Top. Med. Chem.* **2005**, *5*, 687–705.

(14) Chakrapani, H.; Bartberger, M. D.; Toone, E. J. *C*-Nitroso Donors of Nitric Oxide. *J. Org. Chem.* **2009**, *74*, 1450–1453.

(15) Bethke, P. C.; Libourel, I. G. L.; Reinöhl, V.; Jones, R. L. Sodium Nitroprusside, Cyanide, Nitrite, and Nitrate Break Arabidopsis Seed Dormancy in a Nitric Oxide-Dependent Manner. *Planta* **2006**, *223*, 805–812.

(16) Ghosh, K.; Eroy-Reveles, A. A.; Avila, B.; Holman, T. R.; Olmstead, M. M.; Mascharak, P. K. Reactions of NO with Mn(II) and Mn(III) Centers Coordinated to Carboxamido Nitrogen: Synthesis of a Manganese Nitrosyl with Photolabile NO. *Inorg. Chem.* **2004**, *43*, 2988–2997.

(17) Ford, P. C.; Bourassa, J.; Miranda, K.; Lee, B.; Lorkovic, I.; Boggs, S.; Kudo, S.; Laverman, L. Photochemistry of Metal Nitrosyl Complexes. Delivery of Nitric Oxide to Biological Targets. *Coord. Chem. Rev.* **1998**, *171*, 185–202.

(18) Wright, A. M.; Hayton, T. W. Recent Developments in Late Metal Nitrosyl Chemistry. *Comments Inorg. Chem.* **2012**, *33*, 207–248.

(19) Wright, A. M.; Zaman, H. T.; Wu, G.; Hayton, T. W. Nitric Oxide Release from a Nickel Nitrosyl Complex Induced by One-Electron Oxidation. *Inorg. Chem.* **2013**, *52*, 3207–3216.

(20) Hayton, T. W.; Legzdins, P.; Sharp, W. B. Coordination and Organometallic Chemistry of Metal−NO Complexes. *Chem. Rev.* **2002**, *102*, 935–992.

(21) Münzel, T.; Daiber, A.; Mülsch, A. Explaining the Phenomenon of Nitrate Tolerance. *Circ. Res.* **2005**, *97*, 618–628.

(22) Cederqvist, B.; Persson, M. G.; Gustafsson, L. E. Direct Demonstration of NO Formation in Vivo from Organic Nitrites and Nitrates, and Correlation to Effects on Blood Pressure and to in Vitro Effects. *Biochem. Pharmacol.* **1994**, *47*, 1047–1053.

(23) Hrabie, J. A.; Keefer, L. K. Chemistry of the Nitric Oxide-Releasing Diazeniumdiolate ("Nitrosohydroxylamine") Functional Group and Its Oxygen-Substituted Derivatives. *Chem. Rev.* **2002**, *102*, 1135–1154.

(24) Hwu, J. R.; Yau, C. S.; Tsay, S.-C.; Ho, T.-I. Thermal- and Photo-Induced Transformations of *N*-Aryl-*N*-Nitrosohydroxylamine Ammonium Salts to Azoxy Compounds. *Tetrahedron Lett.* **1997**, *38*, 9001–9004.

(25) Hou, Y.; Xie, W.; Janczuk, A. J.; Wang, P. G. *O*-Alkylation of Cupferron: Aiming at the Design and Synthesis of Controlled Nitric Oxide Releasing Agents. *J. Org. Chem.* **2000**, *65*, 4333–4337.

(26) Hou, Y.; Xie, W.; Ramachandran, N.; Mutus, B.; Janczuk, A. J.; Wang, P. G. *O*-Alkylation Chemistry of Neocupferron. *Tetrahedron Lett.* **2000**, *41*, 451–456.

(27) Keefer, L. K.; Flippen-Anderson, J. L.; George, C.; Shanklin, A. P.; Dunams, T. M.; Christodoulou, D.; Saavedra, J. E.; Sagan, E. S.; Bohle, D. S. Chemistry of the Diazeniumdiolates I. Structural and Spectral Characteristics of the $[N(O)NO]^-$ Functional Group. *Nitric Oxide* **2001**, *5*, 377–394.

(28) DeRosa, F.; Kibbe, M. R.; Najjar, S. F.; Citro, M. L.; Keefer, L. K.; Hrabie, J. A. Nitric Oxide-Releasing Fabrics and Other Acrylonitrile-Based Diazeniumdiolates. *J. Am. Chem. Soc.* **2007**, *129*, 3786–3787.

(29) Shirota, F. N.; DeMaster, E. G.; Lee, M. J. C.; Nagasawa, H. T. Generation of Nitric Oxide and Possibly Nitroxyl by Nitrosation of Sulfohydroxamic Acids and Hydroxamic Acids. *Nitric Oxide* **1999**, *3*, 445–453.

(30) Southan, G. J.; Srinivasan, A. Nitrogen Oxides and Hydroxyguanidines: Formation of Donors of Nitric and Nitrous Oxides and Possible Relevance to Nitrous Oxide Formation by Nitric Oxide Synthase. *Nitric Oxide* **1998**, *2*, 270–286.

(31) Keefer, L. K. Fifty Years of Diazeniumdiolate Research. From Laboratory Curiosity to Broad-Spectrum Biomedical Advances. *ACS Chem. Biol.* **2011**, *6*, 1147–1155.

(32) Blangetti, M.; Fraix, A.; Lazzarato, L.; Marini, E.; Rolando, B.; Sodano, F.; Fruttero, R.; Gasco, A.; Sortino, S. A Non-metal-Containing Nitric Oxide Donor Activated with Single-Photon Green Light. *Chem. – Eur. J.* **2017**, *23*, 9026–9029.

(33) Makris, C.; Carmichael, J. R.; Zhou, H.; Butler, A. *C*-Diazeniumdiolate Graminine in the Siderophore Gramibactin Is Photoreactive and Originates from Arginine. *ACS Chem. Biol.* **2022**, *17*, 3140–3147.

(34) Hrabie, J. A.; Arnold, E. V.; Citro, M. L.; George, C.; Keefer, L. K. Reaction of Nitric Oxide at the β-Carbon of

Enamines. A New Method of Preparing Compounds Containing the Diazeniumdiolate Functional Group. *J. Org. Chem.* **2000**, *65*, 5745–5751.

(35) Arnold, E. V.; Citro, M. L.; Saavedra, E. A.; Davies, K. M.; Keefer, L. K.; Hrabie, J. A. Mechanistic Insight into Exclusive Nitric Oxide Recovery from a Carbon-Bound Diazeniumdiolate. *Nitric Oxide* **2002**, *7*, 103–108.

(36) Arnold, E. V.; Citro, M. L.; Keefer, L. K.; Hrabie, J. A. A Nitric Oxide-Releasing Polydiazeniumdiolate Derived from Acetonitrile. *Org. Lett.* **2002**, *4*, 1323–1325.

(37) Baeza Cinco, M. Á.; Kräh, S.; Guzman, C. F.; Wu, G.; Hayton, T. W. Photolytic or Oxidative Fragmentation of Trityl Diazeniumdiolate ($O_2N_2CPh_3^-$): Evidence for Both C–N and N–N Bond Cleavage. *Inorg. Chem.* **2022**, *61*, 14924–14928.

(38) Hrabie, J. A.; Citro, M. L.; Chmurny, G. N.; Keefer, L. K. Carbon-Bound Diazeniumdiolates from the Reaction of Nitric Oxide with Amidines. *J. Org. Chem.* **2005**, *70*, 7647–7653.

(39) Southan, G. J.; Srinivasan, A.; Keefer, L. K.; George, C.; Fales, H. M. *N* -Nitrosated *N* -Hydroxyguanidines Are Nitric Oxide-Releasing Diazeniumdiolates. *Chem. Commun.* **1998**, 1191–1192.

(40) Ishwara Bhat, J.; Clegg, W.; Maskill, H.; J. Elsegood, M. R.; D. Menneer, I.; C. Miatt, P. *N* -Nitroso- *N* , *O* -Dialkylhydroxylamines: Preparation, Structure, and Mechanism of the Hydronium Ion Catalysed Solvolytic Nitrous Oxide Extrusion Reaction. *J. Chem. Soc. Perkin Trans. 2* **2000**, 1435–1446.

(41) Furman, N. H.; Mason, W. B.; Pekola, J. S. Extraction of Cupferrates. *Anal. Chem.* **1949**, *21*, 1325–1330.

(42) Popov, A. I.; Wendlandt, W. W. Cupferron and Neocupferron Complexes of Rare Earth Elements. *Anal. Chem.* **1954**, *26*, 883–886.

(43) Van der Helm, D.; Merritt, L. L.; Degeilh, R.; MacGillavry, C. H. The Crystal Structure of Iron Cupferron $Fe(O_2N_2C_6H_5)_3$. *Acta Crystallogr.* **1965**, *18*, 355–362.

(44) Klebe, G.; Hadicke, E.; Boehn, K. H.; Reuther, W.; Hickmann, E. Die Molekül- Und Kristallstruktur Der Kupfer-, Aluminium-Und Kaliumkomplexe Des Cyclohexyl-Hydroxy-Diazeniumoxids1. *Z. Für Krist. - Cryst. Mater.* **1996**, *211*, 798–803.

(45) Lymar, S. V.; Shafirovich, V. Photoinduced Release of Nitroxyl and Nitric Oxide from Diazeniumdiolates. *J. Phys. Chem. B* **2007**, *111*, 6861–6867.

(46) Poskrebyshev, G. A.; Shafirovich, V.; Lymar, S. V. Disproportionation Pathways of Aqueous Hyponitrite Radicals ($HN_2O_2^{\bullet}/N_2O_2^{\bullet-}$). *J. Phys. Chem. A* **2008**, *112*, 8295–8302.

(47) Hosseininasab, V.; DiMucci, I. M.; Ghosh, P.; Bertke, J. A.; Chandrasekharan, S.; Titus, C. J.; Nordlund, D.; Freed, J. H.; Lancaster, K. M.; Warren, T. H. Lewis Acid-Assisted Reduction of Nitrite to Nitric and Nitrous Oxides via the Elusive Nitrite Radical Dianion. *Nat. Chem.* **2022**, *14*, 1265–1269.

(48) Cirera, J.; Ruiz, E.; Alvarez, S. Continuous Shape Measures as a Stereochemical Tool in Organometallic Chemistry. *Organometallics* **2005**, *24*, 1556–1562.

(49) L, M. C.; Clegg, W.; Demirtas, I.; Elsegood, M. R. J.; Haider, J.; Maskill, H.; Miatt, P. C. *N*-Tritylhydroxylamines: Preparations, Structures, Base Strengths, and Reactions with Nitrous Acid and Perchloric Acid. *J. Chem. Soc. Perkin Trans. 2* **2001**, 1742–1747.

(50) Xie, L.-H.; Hou, X.-Y.; Hua, Y.-R.; Tang, C.; Liu, F.; Fan, Q.-L.; Huang, W. Facile Synthesis of Complicated 9,9-Diarylfluorenes Based on $BF_3{\cdot}Et_2O$-Mediated Friedel−Crafts Reaction. *Org. Lett.* **2006**, *8*, 3701–3704.

(51) Stauffer, M.; Sakhaei, Z.; Greene, C.; Ghosh, P.; Bertke, J. A.; Warren, T. H. Mechanism of *O*-Atom Transfer from Nitrite: Nitric Oxide Release at Copper(II). *Inorg. Chem.* **2021**, *60*, 15968–15974.

(52) Touchton, A. J.; Wu, G.; Hayton, T. W. Generation of a Ni_3 Phosphinidene Cluster from the Ni(0) Synthon, $Ni(\eta_3\text{-}CPh_3)_2$. *Organometallics* **2020**, *39*, 1360–1365.

(53) Wright, A. M.; Wu, G.; Hayton, T. W. Formation of N_2O from a Nickel Nitrosyl: Isolation of the Cis-$[N_2O_2]^{2-}$ Intermediate. *J. Am. Chem. Soc.* **2012**, *134*, 9930–9933.

(54) Wright, A. M.; Zaman, H. T.; Wu, G.; Hayton, T. W. Mechanistic Insights into the Formation of N_2O by a Nickel Nitrosyl Complex. *Inorg. Chem.* **2014**, *53*, 3108–3116.

(55) Wright, A. M.; Hayton, T. W. Understanding the Role of Hyponitrite in Nitric Oxide Reduction. *Inorg. Chem.* **2015**, *54*, 9330–9341.

(56) McBride, D. W.; Stafford, S. L.; Stone, F. G. A. Chemistry of the Metal Carbonyls. XVI. Synthesis of Dicarbonyldinitrosyliron(0). *Inorg. Chem.* **1962**, *1*, 386–388.

(57) Bitterwolf, T. E.; Steele, B. Facile Synthesis of $Fe(NO)_2L_2$ Compounds, Where L=phosphines and Phosphites. *Inorg. Chem. Commun.* **2006**, *9*, 512–513.

(58) Speelman, A. L.; Zhang, B.; Silakov, A.; Skodje, K. M.; Alp, E. E.; Zhao, J.; Hu, M. Y.; Kim, E.; Krebs, C.; Lehnert, N. Unusual Synthetic Pathway for an $\{Fe(NO)_2\}_9$ Dinitrosyl Iron Complex (DNIC) and Insight into DNIC Electronic Structure via Nuclear Resonance Vibrational Spectroscopy. *Inorg. Chem.* **2016**, *55*, 5485–5501.

(59) Tsai, M.-L.; Tsou, C.-C.; Liaw, W.-F. Dinitrosyl Iron Complexes (DNICs): From Biomimetic Synthesis and Spectroscopic Characterization toward Unveiling the Biological and Catalytic Roles of DNICs. *Acc. Chem. Res.* **2015**, *48*, 1184–1193.

(60) Atkinson, F. L.; Blackwell, H. E.; Brown, N. C.; Connelly, N. G.; Crossley, J. G.; Orpen, A. G.; Rieger, A. L.; Rieger, P. H. Synthesis of the 17-Electron Cations $[FeL(L')(NO)_2]^+$(L, L′= PPh_3, $OPPh_3$): Structure and Bonding in Four-Co-Ordinate Metal Dinitrosyls, and Implications for the Identity of Paramagnetic Iron Dinitrosyl Complex Catalysts. *J. Chem. Soc. Dalton Trans.* **1996**, 3491–3502.

(61) Butler, A. R.; Megson, I. L. Non-Heme Iron Nitrosyls in Biology. *Chem. Rev.* **2002**, *102*, 1155–1166.

(62) Vanin, A. F.; Serezhenkov, V. A.; Mikoyan, V. D.; Genkin, M. V. The 2.03 Signal as an Indicator of Dinitrosyl–Iron Complexes with Thiol-Containing Ligands. *Nitric Oxide* **1998**, *2*, 224–234.

(63) Tsou, C.-C.; Lu, T.-T.; Liaw, W.-F. EPR, UV−Vis, IR, and X-Ray Demonstration of the Anionic Dimeric Dinitrosyl Iron Complex $[(NO)_2Fe(\mu\text{-}S^tBu)_2Fe(NO)_2]^-$: Relevance to the Products of Nitrosylation of Cytosolic and Mitochondrial Aconitases, and High-Potential Iron Proteins. *J. Am. Chem. Soc.* **2007**, *129*, 12626–12627.

(64) Chiang, C.-Y.; Miller, M. L.; Reibenspies, J. H.; Darensbourg, M. Y. Bismercaptoethanediazacyclooctane as a N_2S_2 Chelating Agent and Cys−X−Cys Mimic for Fe(NO) and $Fe(NO)_2$. *J. Am. Chem. Soc.* **2004**, *126*, 10867–10874.

(65) Borodulin, R. R.; Kubrina, L. N.; Shvydkiy, V. O.; Lakomkin, V. L.; Vanin, A. F. A Simple Protocol for the Synthesis of Dinitrosyl Iron Complexes with Glutathione: EPR, Optical, Chromatographic and Biological Characterization of Reaction Products. *Nitric Oxide* **2013**, *35*, 110–115.

(66) Lu, T.-T.; Chiou, S.-J.; Chen, C.-Y.; Liaw, W.-F. Mononitrosyl Tris(Thiolate) Iron Complex $[Fe(NO)(SPh)_3]^-$ and Dinitrosyl Iron Complex $[(EtS)_2Fe(NO)_2]^-$: Formation

Pathway of Dinitrosyl Iron Complexes (DNICs) from Nitrosylation of Biomimetic Rubredoxin $[Fe(SR)_4]^{2-/1-}$ (R = Ph, Et). *Inorg. Chem.* **2006**, *45*, 8799–8806.

(67) Tsai, M.-L.; Chen, C.-C.; Hsu, I.-J.; Ke, S.-C.; Hsieh, C.-H.; Chiang, K.-A.; Lee, G.-H.; Wang, Y.; Chen, J.-M.; Lee, J.-F.; Liaw, W.-F. Photochemistry of the Dinitrosyl Iron Complex $[S_5Fe(NO)_2]^-$ Leading to Reversible Formation of $[S_5Fe(\mu\text{-}S)_2FeS_5]^{2-}$: Spectroscopic Characterization of Species Relevant to the Nitric Oxide Modification and Repair of [2Fe−2S] Ferredoxins. *Inorg. Chem.* **2004**, *43*, 5159–5167.

(68) Weil, J. A.; Bolton, J. R. *Electron Paramagnetic Resonance: Elementary Theory and Practical Applications*; Wiley, 2007.

(69) Tzerpos, N. I.; Zarkadis, A. K.; Kreher, R. P.; Repas, L.; Lehnig, M. Diphenylpyridylmethyl Radicals. Part 1. Synthesis, Dimerization and ENDOR Spectroscopy of Diphenyl(2-, 3- or 4-Pyridyl)Methyl Radicals; Bond Dissociation Enthalpies of Their Dimers. *J. Chem. Soc. Perkin Trans. 2* **1995**, 755–761.

(70) Baeza Cinco, M. Á.; Wu, G.; Telser, J.; Hayton, T. W. Structural and Spectroscopic Characterization of a Zinc-Bound *N*-Oxyphthalimide Radical. *Inorg. Chem.* **2022**, *61*, 13250–13255.

(71) Hung, C.-H.; Peng, C.-H.; Shen, Y.-L.; Wang, S.-L.; Chuang, C.-H.; Lee, H. M. Preparation and Oxygenation of Cobalt *N*-Confused Porphyrin Nitrosyl Complexes. *Eur. J. Inorg. Chem.* **2008**, *2008*, 1196–1199.

(72) Brock, C. P.; Collman, J. P.; Dolcetti, G.; Farnham, P. H.; Ibers, J. A.; Lester, J. E.; Reed, C. A. Bent vs. Linear Nitrosyl Paradox. Infrared and X-Ray Photoelectron Spectra of Dichloronitrosylbis(L)Cobalt(II) and Crystal Structure with L = Diphenylmethylphosphine. *Inorg. Chem.* **1973**, *12*, 1304–1313.

(73) Kunkely, H.; Vogler, A. Photoredox Reaction of Iron(III) Cupferronate. Release of NO Induced by Ligand-to-Metal Charge Transfer Excitation. *Inorganica Chim. Acta* **2003**, *346*, 275–277.

(74) Gomberg, M. TRIPHENYLMETHYL. XXII. ETHERS OR OXIDES IN THE TRIPHENYLMETHANE SERIES. *J. Am. Chem. Soc.* **1913**, *35*, 200–210.

(75) Johnson, A. L. New Reaction of (Diethylamino)Sulfur Trifluoride: Bis(Diphenylmethyl) Ethers as Dehydration Products of (Diethylamino)Sulfur Trifluoride and Diarylcarbinols. *J. Org. Chem.* **1982**, *47*, 5220–5222.

(76) Maekawa, T.; Sekizawa, H.; Itami, K. Controlled Alcohol–Carbonyl Interconversion by Nickel Catalysis. *Angew. Chem. Int. Ed.* **2011**, *50*, 7022–7026.

Photolysis of the trityl diazeniumdiolate complexes $[M(O_2N_2CPh_3)_3]^-$ (M = Fe, Co) led to nitric oxide formation in 1 and 10% yields, respectively.